The Dynamics of End-to-End Cyclization in Polystyrene Probed by Pyrene Excimer Formation

Mitchell A. Winnik* and T. Redpath

Lash Miller Laboratories, Department of Chemistry and Erindale College, University of Toronto, Toronto, Canada M5S 1A1

D. H. Richards

P.E.R.M.E., Waltham Abbey, Essex, England EN9 1BP. *Received July 17, 1979*

ABSTRACT: Pyrene excimer formation is an excellent probe of the kinetics of end-to-end cyclization of terminally substituted polystyrene. The 200-ns fluorescence lifetime permits one to study, using a combination of steady-state and time-resolved measurements, rates of cyclization that occur on the microsecond time scale. A log-log plot of the rate constant for excimer formation $\langle k_1 \rangle$ vs. $\bar{M}_n$ gives a slope of −1.6, but this result must be corrected, both for the mass of the pyrenes attached to the chain ends and for the polydispersity of the polystyrene samples. The nature of this correction is discussed. The corrected value of the rate constant for end-to-end cyclization depends upon the degree of polymerization N of the polymer according to $N^{-1.35}$ for samples with $3900 \leq \bar{M}_n \leq 27\,000$. This value of γ is smaller than that predicted by current theories of polymer cyclization dynamics.

When two aromatic chromophores capable of undergoing a photochemical reaction are attached to the ends of a polymer chain, the chain imposes constraints on that reaction. When the chain is short, structural feactures associated with interactions between neighboring monomer units limit the relative orientations of the chromophores and perturb the nature of the photochemical reaction. When the chains are long, the conformational flexibility of the polymer permits all possible relative orientations of the terminal chromophores to occur, as in bimolecular reactions, but the rate of the photoreaction between the chromophores is limited by the cyclization properties of the chain. Inefficient chemical reactions have rates proportional to the cyclization probability of the chain. Photochemical reactions that occur on every encounter between the chromophores have rates governed by the cyclization dynamics of the chain.

These concepts apply to nonphotochemical reactions as well. Polymer chemists have carried out kinetic and equilibrium studies of a number of cyclization reactions related to polymer cyclization probability.[1] Others have carried out numerous studies of cyclization and ring closure reactions of molecules containing short chains, both under statistical and dynamic control.[2] There is less known about dynamically controlled end-to-end cyclization in long polymers. These measurements have become of particular importance in polymer chemistry because of the great advances that have been made over the last 7 years in the theory of polymer dynamics.

Beginning with the classic papers of Wilemski and Fixman,[3] there has been essentially a revolution in the theoretical description of end-to-end cyclization dynamics in polymers. Important contributions by Fixman,[3a,b] Doi,[4] Brereton and Rusli,[5] and Perico and Cuniberti[6] have focused attention on this relaxation mode of long polymers and provided a format whereby fluorescence quenching or similar kinds of photochemical studies on suitable terminally substituted polymers could provide important tests of these theoretical ideas.

In spite of the widely recognized importance of subjecting these theoretical descriptions to critical experimental scrutiny and providing the quantitative basis for revisions and refinements in the theory, there have been few experimental studies of end-to-end cyclization dynamics of polymers in solution.[7] In order to appreciate why it has taken so long for quantitative experimental work to appear, it is worth looking at the complexity of the problem and the demands it places upon experimental research groups.

All of the theoretical treatments suggest that the rate constant for end-to-end cyclization k_{cy} should be a function of the molecular weight (M) or degree of polymerization (N) of the polymer according to

$$k_{cy} = AM^{-\gamma} = BN^{-\gamma} \tag{1}$$

The rate constant for end-to-end cyclization provides a quantitative measure of the magnitude of the slowest relaxation mode of the polymer. Depending upon the details of the theoretical treatment, γ is anticipated to fall in the region of $1.5 \leq \gamma \leq 2.0$. Other factors which should affect the rate constant for end-to-end cyclization are the polymer structure, the "goodness" of the solvent, and hydrodynamic features associated with solvent viscosity. These factors are thought to affect the proportionality constants, although the way in which excluded volume enters into chain dynamics is still unclear.

The experimentalist is charged with carrying out experiments which permit k_{cy} to be calculated, as a function of molecular weight and solvent, for a variety of different polymers, with sufficient precision that A, B, and γ may be known with some confidence. This requires the following: (i) polymers functionalized on both ends with appropriate chromophores for photochemical or photophysical studies; (ii) polymers of exceptionally narrow molecular weight distribution; (iii) polymers and solvents of high purity, free from adventitious quenchers or fluorescent impurities; and (iv) rather sophisticated equipment for transient spectroscopic measurements on nanosecond and microsecond time scales.

These are demanding criterea which have been met in their entirety only for a few examples of relatively short-chain-containing molecules.

Because of its long excited singlet lifetime, the pyrene chromophore[7,8] is an attractive choice for studying cyclization dynamics in polymers. Simple alkyl pyrene derivatives fluoresce intensely at wavelengths of 370 to 450 nm. In addition, photoexcited pyrene has the remarkable property of forming a complex (an excimer) with a second, ground state pyrene, and this complex gives a strong broad fluorescence red shifted from the pyrene fluorescence band.[8] Consequently, a polymer substituted at both ends with appropriate pyrene derivatives offers the possibility

0024-9297/80/2213-0328$01.00/0

that one can study end-to-end cyclization by observing the time dependence of the change in fluorescence from the blue-violet pyrene fluorescence to the blue-green excimer fluorescence on a nanosecond and microsecond time scale.

The first study of intramolecular pyrene excimer formation in small molecules was reported by Zachariasse.[9] He has devoted many years to the study of the series of molecules 1-pyrene-$(CH_2)_n$-1-pyrene for many values of n between 1 and 32. His observations indicate that the extent of the excimer formation depends both on the conformational and the dynamic properties of the hydrocarbon chains,[9b] showing in particular strong inhibition of intramolecular excimer formation for n = 5 to 8. These correspond to chain lengths for which end-to-end cyclization is known to be difficult.[10]

Cuniberti and Perico[7] recognized the power of pyrene excimer formation as a probe of end-to-end cyclization dynamics in polymers and prepared a series of pyrene end-capped poly(ethylene oxide) polymers. They carried out careful measurements of pyrene "monomer" (local excited state) and pyrene excimer fluorescence intensities for dilute solutions of these molecules and demonstrated that the time scale of excimer formation was comparable to that of the pyrene excited singlet lifetime. Unfortunately, they did not have access to equipment for measuring these lifetimes. They were thus unable to calculate mean rate constants for the end-to-end cyclization process.

Stiff polymers of a high degree of polymerization ought to undergo very slow cyclization. Here pyrene excimer probes may be unsuitable and probes based upon triplet state reactions offer advantages. Mita[11] has examined triplet–triplet annihilation reactions between two anthracenes attached to the ends of polystyrene of degree of polymerization N = 300–1000. He finds that the apparent rate constant for end-to-end cyclization is not very sensitive to chain length. Measuring triplet–triplet annihilation rates is exceptionally difficult.[12] Separating intra- from bimolecular processes in these measurements is even more difficult, particularly at 10^{-4} M where most of these studies were carried out.

In this paper we report our first results on the study of end-to-end cyclization in polystyrene in very dilute [10^{-6} M] solution in toluene, using excimer formation between pyrenes attached to the chain termini to determine values of k_{cy}. Our measurements, with polystyrene samples of $\bar{M}_n$ between 3900 and 27 000, provide good values of k_{cy} and lead to the conclusion that in this molecular weight range γ = 1.35. This value is somewhat smaller in absolute magnitude than that predicted by any of the foremen-tioned theories. More important, that exact value of γ determined depends in a critical way on how the data are processed. These difficulties are related to the four factors listed above, particularly molecular weight dispersity.

In the sections below we present our results and discuss the sensitivity of our conclusions to the way in which we treat our data. Finally we comment on the implications of our conclusions on current theories of cyclization dynamics.

Experimental Section

Polymer Synthesis. Polystyrene samples were prepared by anionic polymerization in THF, under argon, using naphthylpotassium as the initiator. The living ends were quenched with excess ethylene oxide, and the resulting gel was treated with glacial acetic acid once all trace of the deep red color of the benzyl carbanion had disappeared. The hydroxy-terminated polymer was precipitated into methanol and purified by reprecipitation from toluene solution into excess methanol.

4-(1′-Pyrene)butyryl chloride was prepared from the corresponding acid by treatment with excess thionyl chloride in benzene. It was recrystallized from toluene–hexane mixtures to give pale yellow crystals, mp 89–90 °C.

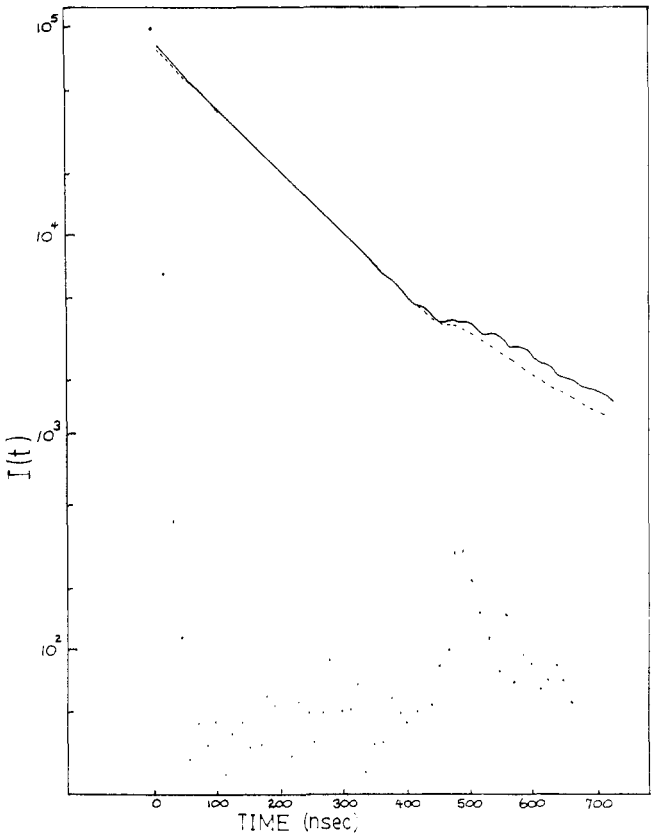

Figure 1. Plot of log I (intensity) vs. time obtained by single photon counting for $\bar{M}_n$ 6200 and compared with that for lamp decay. The blip at 400 ns is due to double pulsing of the phototube. The dashed curve refers to the theoretical exponential decay curve convoluted with the lamp profile (···). The solid line refers to the actual data.

For functionalization of the polymer, 100 mg to 200 mg portions of the polymer were mixed with a five- to tenfold molar excess of pyrenebutyryl chloride and dissolved in 5 mL of dry toluene. To this was added 0.5 mL of dry pyridine. The reaction mixture was stirred 3–5 days in the dark and worked up by reprecipitating the filtered solution into methanol. Crude yields were essentially quantitative. In spite of repeated reprecipitations, analysis by gel permeation chromatography (GPC) showed the presence of UV absorbing low molecular weight impurities. Consequently, 20 mg to 30 mg portions of the polymer were purified by GPC, using the same microstyragel columns as for the mass distribution analysis. One polymer of nominal $\bar{M}_n$ = 25 000 was fractionated by this method to give two polymers of $\bar{M}_n$ = 24 150 and 27 100, respectively.

Polymer Analysis. Polymers were analyzed by gel permeation chromatography using a Waters Associates Model High Pressure Liquid Chromatograph and microstyragel columns of pore size 10^4, 10^3, and 500 Å, respectively, calibrated with appropriate polystyrene standards. Mole fractions at each mass were inferred using the method of Tung,[13] and $\bar{M}_n$ and $\bar{M}_w$ were calculated from these distributions.

$\bar{M}_n$ could also be calculated by end group analysis. Both UV absorption analysis of pyrene absorption and, for low molecular weight polymers, ^{1}H NMR analysis of pyrene and ester O–CH_2 resonances suggested that greater than 90% of the polymers carried pyrenes on both ends.

Sample Preparation. Samples were weighed on a microbalance and dissolved in toluene (purified by refluxing over potassium followed by fractional distillation). These solutions of concentration 1–2 × 10^{-6} M were placed in cylindrical Pyrex cells, which were outgassed by four freeze–pump–thaw cycles at 10^{-5} Torr and sealed under vacuum.

Emission Spectra. Emission spectra were taken on a "Spex Fluorolog" photon counting spectrometer and also on a "Fica

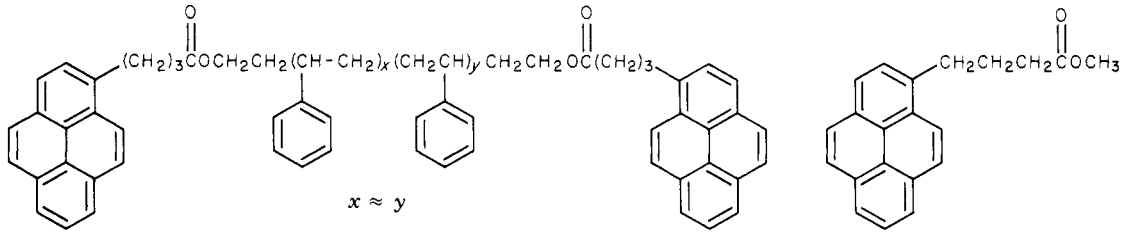

1 2

Fluorimètre absolu et différentiel", the latter providing corrected spectra. The spectra were taken in Leuven, Belgium, in the Department of Chemistry at the Katholeike Univesiteit Leuven. Since the photomultiplier in the Fica has very poor response to signals at $\lambda > 550$ nm, all quantitative interpretations based upon weak emissions to the red of 500 nm were made using traces taken on the former spectrometer.

Lifetime Measurements. Fluorescence lifetimes were measured by the time-correlated single photon counting technique.[14] Decay traces were exponential over one to two decades of the fluorescence intensity, with ubiquitous positive deviations in the tail of the decay curve. A typical decay trace and the corresponding lamp curve are shown in Figure 1. The positive deviations are believed to be due to the longer lifetime of fluorescence of the higher molecular weight species within the sample, and strictly speaking, the lifetimes reported for each sample are mean lifetimes $\langle \tau \rangle$ averaged over the individual molecular weight polymers contributing to the decay.

Excimer decay times in the low molecular weight polymers ($\bar{M}_n$ = 3900–6200) were identical with those of the corresponding pyrene monomer fluorescence in the sample.

Results and Discussion

The polymers we prepared for this study of end-to-end cyclization dynamics have the structure 1 below. Both NMR for low molecular weight samples and UV absorption spectroscopy, in combination with the GPC determination of $\bar{M}_n$, gave indications of quantitative esterification of the chain ends. The most serious problem encountered in the preparation of 1 was its purification. Repeated precipitations failed to remove all of the low molecular weight fluorescent impurities. We chose, therefore, to purify small quantitites of our polymers by gel-permeation chromatography.

Fluorescence studies of 1 were carried out in toluene at 1×10^{-6} M polymer concentration. At this concentration, literature values of the intrinsic viscosity of polystyrene in toluene suggest that the polymers are about 2–3 orders of magnitude below the concentration at which bimolecular chain entanglements become important.[15] In addition, a model compound for our studies, the methyl ester 2 of pyrenebutyric acid, shows no detectable excimer formation at this concentration. Since 2 must form excimers in a bimolecular reaction, this result indicates that in 1, bimolecular excimer formation is unimportant at 1×10^{-6} M, and all of the observations reported here refer to intramolecular processes.

The emission spectra of the pyrene-substituted polymers are shown in Figure 1 and compared with that of the methyl ester of pyrenebutyric acid. At low concentrations (1.2×10^{-6} M), the fluorescence spectrum of 2 resembles a typical pyrene fluorescence spectrum. The terminally substituted polymers also show this pyrene fluorescence but in addition give a new emission as a broad structure band centered at 480 nm. This new emission is due to pyrene excimer formation.[8] The pyrene excimer is an electronically excited complex between a photoexcited pyrene and a ground state pyrene. This complex is thought to have a sandwich-like arrangement of the two pyrenes. Under the high dilution conditions of our experiments, these excimers are formed exclusively in an intramolecular reaction: the intensity of pyrene excimer fluorescence I_E relative to pyrene "monomer" fluorescence I_M is a measure of the dynamics of end-to-end cyclization. Pyrene fluorescence lifetimes and measured I_E/I_M ratios are presented in Table I.

Table I
Molecular Weights and Fluorescence Lifetimes of Polystyrene Samples Terminally Substituted with Pyrene

polymer	$\bar{M}_n$[a]	$\bar{M}_w/\bar{M}_n$[a]	τ, ns	χ^2[b]	rel I_E/I_M
PS 3900	3 900	1.42	110.9	14.6	1.87
PS 4100	4 100	1.25	111.3	10	1.64
PS 6200	6 200	1.42	137.5	9.7	1.00[c]
PS 24K	24 150	1.12	186.2	3.3	0.09
PS 27K	27 100	1.13	186.8	0.95	0.05
methyl ester 2			193.5	1.14	0.00

[a] Determined by GPC. [b] Standard χ^2 displacements in the fluorescence decay curves. [c] Arbitrary reference.

Scheme I

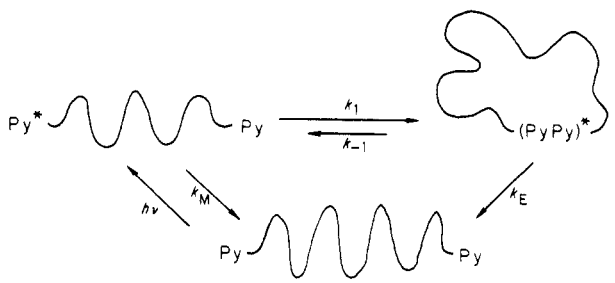

Quantitative determination of the rate constant for end-to-end cyclization requires interpretation of the data in terms of the mechanism of the reaction. Pyrene excimer formation has been studied in detail;[8] Scheme I is consistent with the currently accepted mechanism of excimer formation. Upon irradiation one pyrene becomes excited. It fluoresces or decays radiationlessly with a sum of rate constants k_M. In competition with this decay, it forms the excimer intramolecularly with a rate constant k_1. The excimer can dissociate back to excited pyrene plus ground state pyrene by the process labeled k_{-1}, or it can fluoresce or decay radiationlessly back to the ground state with a sum of rate constants k_E. There is now a vast body of experimental evidence to suggest that excimers are formed at diffusion controlled or encounter controlled rates;[8] hence one can equate k_1 with the rate constant k_{cy} for dynamically controlled end-to-end cyclization. Since the binding energy of the pyrene excimer is large, its dissociation at room temperature does not compete with its decay; at room temperature $k_{-1} \ll k_E$. The "low temperature limit" obtains,[8] and the magnitude of I_E/I_M provides a measure of k_1.

In the low-temperature limit, there are three ways of obtaining the rate constant k_1 from a combination of steady state and transient fluorescence measurements. One depends upon the ability of excimer formation to

Table II
Calculated Mean Rate Constants $\langle k_1 \rangle$ for Intramolecular Excimer Formation

$\bar{M}_n$	$\bar{M}_n'$ [a]	$\langle k_1 \rangle$, s^{-1} from τ [b]	$\langle k_1 \rangle$, s^{-1} from (I_E/I_M) [c]
3 900	3 350	3.85×10^6	3.9×10^6
4 100	3 550	3.82×10^6	3.4×10^6
6 200	5 650	2.1×10^6	2.1×10^6
24 150	23 600	2.0×10^5	2.2×10^5
27 100	26 550	1.8×10^5	1.4×10^5

[a] Calculated from $\bar{M}_n' = \bar{M}_n - 550$. [b] Calculated using eq 3. [c] Calculated using eq 4.

quench monomer fluorescence intensity. The ratio of the quantum yield of pyrene fluorescence if excimer formation were not possible (Φ^0_M) to that actually measured (Φ_M) is related to the rate of excimer formation by the expression

$$\frac{\Phi^0_M}{\Phi_M} - 1 = \frac{k_1}{k_M} = k_1 \tau_{model} \tag{2}$$

Both Φ^0_M and k_M can be determined by reference to the model compound, since $k_M = \tau^{-1}_{model}$ where τ_{model} is the measured fluorescence lifetime of the model compound and Φ^0_M is its fluorescence quantum yield. This is the equation used by Cuniberti and Perico[7] in their analysis of excimer formation of pyrene terminated poly(ethylene oxide). Since they were unable to measure τ_{model}, they could not calculate values for k_{cy}. This expression has the disadvantage that Φ^0_M/Φ_M rapidly approaches 1.0 for long polymers: there is very little precision in the measurement of k_1/k_M.

An expression analogous to (2) can be written in terms of the measured fluorescence lifetimes of the pyrene substituted polymers τ and that of the model compound. Here

$$\frac{1}{\tau} - \frac{1}{\tau_{model}} = k_1 \tag{3}$$

and the rate constant for cyclization can be determined directly. When the polymer is sufficiently long, τ becomes nearly equal to τ_{model}, so that k_1 can be calculated only with poor precision.

Neither of these approaches make use of the excimer emission intensity. Comparison of excimer to monomer emission intensities permits one to write for steady state fluorescence spectra[16] that the ratio of excimer to monomer

$$(I_E/I_M)_1/(I_E/I_M)_2 = k_1(1)/k_1(2) \tag{4}$$

intensities for two polymers is proportional to the ratio of their cyclization rate constants. Since k_1 is easily determined with eq 3 for low molecular weight polymers, eq 4 permits values of k_1 to be obtained when the fraction of excimer formed is very small.

Rate constants calculated from eq 3 and 4 represent mean rate constants $\langle k_1 \rangle$ averaged over the ensemble of chains making up the molecular weight distribution in each polymer. These values are reported in Table II. The rate constant for end-to-end cyclization drops from a value of 3.85×10^6 s^{-1} for $\bar{M}_n = 3900$ to a value of 1.4×10^5 s^{-1} for $\bar{M}_n = 27\,000$. It is interesting to realize that a fluorescence probe with an emissive lifetime of 200 ns permits one, via excimer formation, to measure rates of reactions in the microsecond time domain.

Interpretation of the Rate Constant for Intramolecular Excimer Formation. As discussed in the introduction, theoretical treatments of polymer end-to-end cyclization suggest that the dynamically controlled rate constant for this process should vary according to $k_{cy} = AM^{-\gamma}$. Consequently, a plot of log $\langle k_1 \rangle$ vs. log $\bar{M}_n$ should

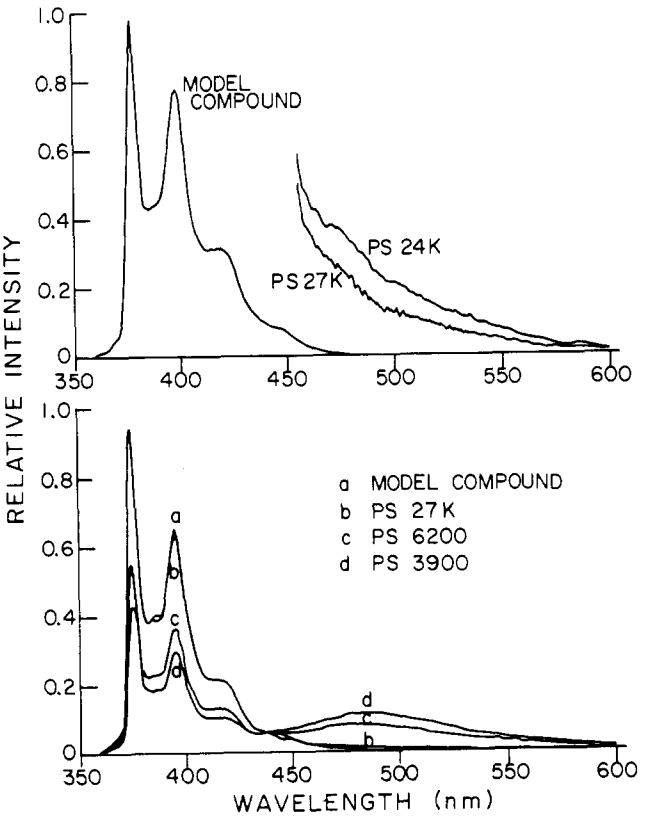

Figure 2. Emission spectra for polystyrene samples 1 compared with that of the model compound 2. Lower curve: corrected spectra of $\bar{M}_n$ 3900, 6200, 27 100 and 2 with the intensity of 2 normalized to that of $\bar{M}_n$ = 27 100 at 385 nm. Upper curve: uncorrected photon counting spectra of $\bar{M}$ = 24 150 and 27 100 and 2 normalized at 385 nm.

provide one measure of the exponent γ. Such a plot leads to the result that log $\langle k_1 \rangle$ = 12.42 − 1.62 log $\bar{M}_n$ (correlation coefficient = 0.998). Since some of the mass associated with each polymer is contained in the terminal pyrene substituent, the $\bar{M}_n$ values determined from the GPC traces should be corrected appropriately. We have decided to define a new number averaged molecular weight $\bar{M}_n' = \bar{M}_n - 550$, in which the molecular mass of the pyrenebutyric acid function is subtracted from the measured molecular weight. Using these corrected values, we find log $\langle k_1 \rangle$ = 11.97 − 1.52 log $\bar{M}_n'$ (correlation coefficient = 0.998).

While these values of the exponent are consistent with those predicted from current theories, the fact that $\langle k_1 \rangle$ is such a strong function of the molecular weight means that the effect of the finite mass distribution in each polymer on $\langle k_1 \rangle$ must be taken into account. This would not be necessary if sufficiently narrow molecular weight fractions were available. One normally thinks of $\bar{M}_w/\bar{M}_n$ ratios of 1.1 to 1.3 as indicating "narrow" molecular weight distributions. As the mass distributions in Figure 2 indicate, these distributions are nonnegligible, and appropriate corrections need to be made.

Renormalized Rate Constants. Calculated values of $\langle k_1 \rangle$ obtained from the experimental measurements of τ and I_E/I_M are not true average rate constants for polymers of any given $\bar{M}_n$, because $\langle k_1 \rangle$ and $\bar{M}_n$ are different functions of the mass distribution in the polymer sample. Since the mass distribution is known, one could renormalize the apparent rate constant $\langle k_1 \rangle$ for each polymer if the dependence of k_{cy} on M were known. We assume that $k_{cy} = AM^{-\gamma}$; consequently for any discrete molecular weight M_i

$$k_{cy,i} = AM_i^{-\gamma} \tag{5}$$

and

$$\langle k_1 \rangle = \sum_{i=1}^{n} k_{cy,i}\chi_i \quad (6)$$

where χ_i is the mole fraction of polymer in the i'th mass interval, and the sum is taken over the n intervals between M_{min} and M_{max}. For any one polymer, $\sum\chi_i = 1.0$.

Using eq 5 and 6, one can use least-squares methods to obtain the best values of both A and γ which give the best fit to all of the data. Because of the presence of the terminal substituents, one must subtract their mass from the molecular weights read off the GPC traces. We optimized A and γ using the expression $k_{cy,i} = A[M_i']^{-\gamma}$. The nonlinear least-squares treatment of the data gives a best value of $\gamma = 1.30$. A linear least-squares minimization of log k_{cy} gives a best value of $\gamma = 1.35$.

Another way of treating the data is to reaverage the molecular weight distribution in each sample so that the average is sensitive to M in the same manner as is k_{cy}. This "excimer averaged" molecular weight can be defined by

$$\bar{M}_{ex} = \sum_{i=1}^{n} k_{cy,i}M_i\chi_i / \sum_{i=1}^{n} k_{cy,i}\chi_i \quad (7)$$

Since k_{cy} is proportional to $M^{-\gamma}$ with $\gamma = 1.35$,

$$\bar{M}_{ex} = \sum\chi_i M_i^{1-\gamma} / \sum\chi_i M_i^{-\gamma} \quad (8)$$

$\bar{M}_{ex}$ corresponds to an inverse moment of the molecular weight distribution of the polymer. Calculated values of $\bar{M}_{ex}$ and renormalized values of k_{cy} are presented in Table III.

The Dependence of k_{cy} upon M. The end-to-end cyclization rate constant k_{cy} shares with the diffusion constant D, the sedimentation coefficient S, and the intrinsic viscosity $[\eta]$ of a polymer the property that it is related to a mean relaxation time of the polymer. Since the relaxation times of a polymer are, for macroscopic deformations, increasing functions of the volume of a polymer, the size of the polymer can be measured in a dynamic experiment. This is a common application to polymers of measurements of D, S, and $[\eta]$.

The end-to-end cyclization rate constant k_{cy} also describes a relaxation of a polymer related to macroscopic chain deformations. This relaxation time τ_{cy} $(=1/k_{cy})$ should also be a function of the volume or molecular dimensions of the polymer. Perico and Cuniberti[6] recognized this similarity in their discussion of the relationship between k_{cy} and $[\eta]$.

A simple and clear way of picturing this dependence was developed by Weill and des Cloizeaux[17] in order to assess the effect of excluded volume on D, S, and $[\eta]$. These authors relate the mean large amplitude relaxation time τ_r of a polymer to two characteristic distances R_G^2 $(\propto\sum_{ij}\langle r_{ij}^2\rangle)$, the mean-squared radius of gyration, and R_D $(\propto\sum_{ij}\langle r_{ij}^{-1}\rangle)$, a dynamic distance ($r_{ij}$ is the distance between the i'th and j'th monomers in a chain of N monomers),

$$\tau_r = 4\pi\eta_0 R_G^2 R_D / k_B T \quad (9)$$

where η_0 is the solvent viscosity, and k_B is the Boltzmann constant. For Θ solvents or where excluded volume is unimportant, $R_G \propto R_D \propto N^{1/2}$. The most controversial aspect of their publication is the suggestion that there exists in good solvents a critical length N_c below which excluded volume is unimportant ($R_G \propto R_D \propto N^{1/2}$) and above which R_G and R_D become different functions of N.

The motion of a polymer chain associated with end-to-end cyclization differs in certain fundamental ways from the chain relaxations which contribute to D, S, and $[\eta]$. For one, cyclization necessarily requires internal rotations to bring the chain ends into proximity. Second, there are indications that cyclization probability $[W(0)]$, an equi-

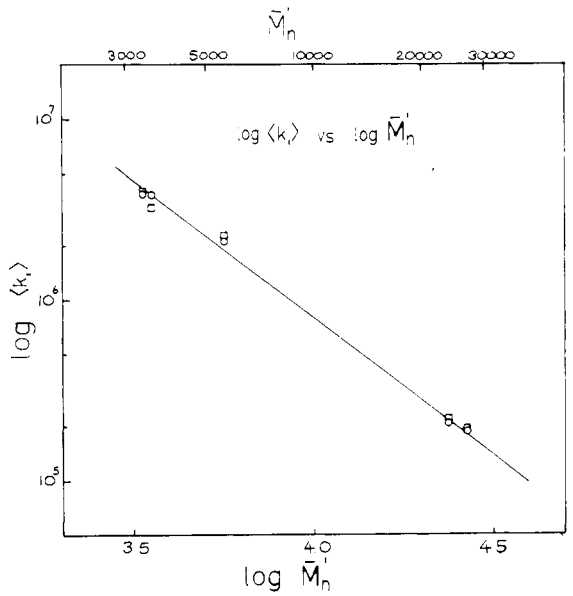

Figure 3. Plot of log $\langle k_1 \rangle$ and log k_{cy} vs. $\bar{M}_n$. Log k_{cy} values are obtained from renormalizing the log $\langle k_1 \rangle$ values according to the molecular weight distribution in each polymer sample according to $k_{cy} = A\bar{M}^{-1.35}$ and assigning this rate constant to the appropriate value of $\bar{M}_n$. See the text.

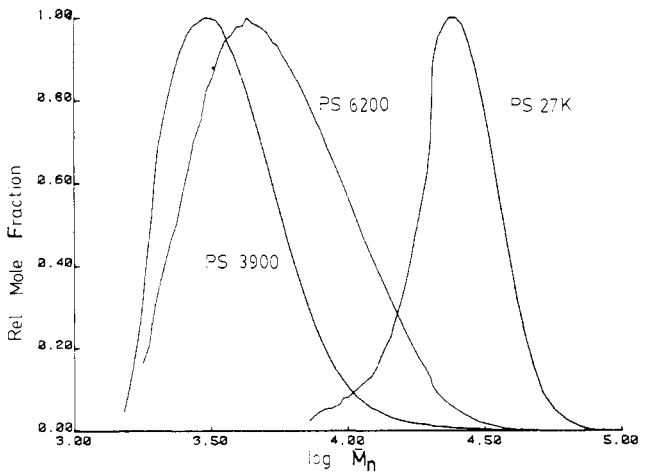

Figure 4. Molecular weight distributions in functionalized polystyrene samples of $\bar{M}_n$ 4100, 6200, and 27 100, plotted as the mole fraction χ vs. the molecular weight M.

Table III
Renormalized Rate Constants for End-to-End Cyclization and "Excimer Averaged" Molecular Weights

		$10^{-5}k$, s^{-1}			
$\bar{M}_n$	$\bar{M}_n'$	k_{cy} (γ = 1.30)[a]	k_{cy} (γ = 1.35)[a]	$\langle k_1 \rangle$	$\bar{M}_{ex}'$[b]
3 900	3 350	40.7	39.7	38.5	2 215
4 100	3 550	33.6	32.6	38.2	2 586
6 200	5 650	23.7	22.7	21.0	3 290
24 150	23 600	2.4	2.1	2.0	19 800
27 100	26 550	2.1	1.9	1.8	21 990

[a] k_{cy} is calculated from $k_{cy} = 9.78 \times 10^4\ M^{-1.30}$ or $k_{cy} = 1.39 \times 10^5\ M^{-1.35}$; see text. [b] Because of the mass of the pyrene substituents on the chain ends, $\bar{M}_{ex}'$ is calculated from $[\Sigma\chi_i(M_i - 550)^{1-\gamma}]/[\Sigma\chi_i(M_i - 550)^{-\gamma}]$, $\gamma = 1.35$.

librium property of the chain, scales according to a different law than R_G in the presence of excluded volume interactions. Since the probability of end-to-end proximity plays a role in determining the dependence of k_{cy} on molecular size, it is worth examining what various theories predict for $W(0)$ as a function of N.

Theories of Cyclization Probability, W(0). In Θ solvents, the distribution function $W(r)$ of the chain ends is Gaussian. Consequently $W(0)$ decreases as $N^{-3/2}$. In good solvents, R_G^2 increases approximately as $N^{6/5}$. If one guesses that $W(0)$ decreases as $(R_G^{-2})^{3/2}$, then one predicts that $W(0)$ decreases as $N^{-9/5}$.

de Gennes' theory[17b] indicates that R_G is proportional to N^{ν}, with $\nu = 0.588$. Although it assumes that a single scaling length suffices to describe cyclization probability, one finds that a second exponent enters into the chain length dependence of $W(0)$. In the presence of excluded volume, $W(0)$ is predicted to depend upon $N^{-1.83}$ whereas τ_r^{-1} in eq 9 is proportional to $N^{-1.76}$.

Series analysis, which involves extrapolations based upon exact enumeration of lattice walks, leads to the conclusion that $W(0)$ decreases as $N^{-23/12}$, i.e., $N^{-1.92}$.[18]

Theories of Cyclization Dynamics. Theories of cyclization dynamics must take account of at least three aspects of the problem: the motion of the chain ends, the connectivity of the chain, and the chemical reaction between the chain ends when the chain ends achieve a reactive configuration. In order for such theories to be tractable, simplifying assumptions need to be made. Various models of cyclization dynamics at various levels of sophistication have been examined.

The simplest of these models is the free particle model of Brereton and Rusli.[5] These authors treat the motion of the chain ends as that of independent particles, which, at equilibrium, satisfy the same Gaussian distance distribution that they would obey if they were connected by a chain of N segments. The authors consider the Brownian motion of the particles and examine the frequency with which one approaches to within some reactive distance a of the other. They find that k_{cy} can be expressed as a product of three terms: an effective cross section $4\pi a^2$ for the reaction, the probability density $W(r)$ of the end-to-end distance, and the mean speed $\langle dR/dt \rangle$ with which the ends approach. According to these authors, the average speed term in their model does not depend upon N. Consequently k_{cy} shows the same dependence on N as does $W(0)$, namely it depends upon $N^{-3/2}$ in Θ solvents and $N^{-9/5}$ in good solvents.

Wilemski and Fixman[3] presented the first theoretical analysis polymer cyclization dynamics. In an important series of papers, these authors developed a formalism for diffusion controlled reactions and showed how a polymer connecting two reactive groups could be incorporated into this formalism. Two simplified models of the polymer chain were considered: Their first model, a harmonic spring [HS] model, treats the polymer as a single harmonic spring connecting the two reactive groups. A "sink term" describes the reaction probability as the groups approach, and the motion of the chain ends satisfies Smoluchowski boundary conditions. For a critical reactive radius a about one of the groups, the rate constant for diffusion controlled reaction for this model, k_{cy}^{HS}, is related to the slowest relaxation time τ_m^{HS} of the chain according to

$$k_{cy}^{HS} \propto (a/R_E)(\tau_m^{HS})^{-1} \quad (10)$$

where R_E^2 is the mean-squared end-to-end length of the polymer.

In commenting on this model, Doi[4] has pointed out that for harmonic springs, $\tau_m^{HS} \propto R_E^2$. Since R_E^2 is proportional to N in the absence of excluded volume, one concludes that $k_{cy}^{HS} \propto N^{-3/2}$.

Table IV
Dynamically Controlled End-to-End Rate Cyclization Rate Constants for Polystyrene Predicted by the Calculations of Perico and Cuniberti[a]

N[b]	360	720	1440	3600
M[b]	47440	74880	150000	374000
R_E, Å[c]	134	190	268	424
$10^{-5}k_{cy}$, s^{-1}	5.6	2.1	0.79	0.21

[a] All data taken from Perico and Cuniberti, ref 6. These refer to a Θ solvent and $\eta/T = 10^{-5}$ P/K where η is the solution viscosity in Poise and T is the absolute temperature; i.e., 0.3 cP at room temperature. [b] N is the degree of polymerization of the polymer, and M is its corresponding molecular weight. [c] R_E is the square root of the mean-squared end-to-end distance for polystyrene.

In the second model of Wilemski and Fixman,[3] the polymer is treated as a Rouse chain of N segments of length b connected by harmonic springs. Wilemski and Fixman calculated values of k_{cy} for both the free draining limit (k_{cy}^{FD}) and the nondraining limit (k_{cy}^{ND}) of hydrodynamic interaction. Their results indicate that for small values of (a/R_E) $[a/R_E \ll 1]$, k_{cy}^{FD} is independent of a and is close in magnitude to the slowest relaxation time τ_m^{FD} of the free-draining Rouse chain. Since τ_m^{FD} is proportional to N^2, k_{cy}^{FD} is expected to be strongly dependent upon the degree of polymerization according to

$$k_{cy}^{FD} \propto (\tau_m^{FD})^{-1} \propto N^{-2} \quad (11)$$

Doi[4] has commented extensively on the differences in cyclization behavior between the harmonic spring model and the free-draining Rouse chain. He has examined a number of assumptions in the Wilemski and Fixman approach and discusses at some length the origin of the (a/R_E) dependence of k_{cy}^{HS} and its absence for k_{cy}^{FD}.

Doi[4d] has also carried out a computer simulation of end-to-end cyclization dynamics using an off-lattice model similar in conception to that first developed by Verdier and Stockmayer.[19] This model has features in common with the free-draining Rouse chain. Values of k_{cy} calculated from this model for various values of (a/R_e) seem to approach a dependence upon N^{-2}, although for the chain lengths examined $[N \leq 70]$ this asymptotic behavior was not yet reached.

Wilemski and Fixman[3] also extended their treatment to include both excluded volume effects and also nondrainng hydrodynamic interactions on the Rouse chain. Calculations of k_{cy}^{ND} were carried out for the nondraining Rouse chain in the absence of excluded volume with the result that

$$k_{cy}^{ND}/k_{cy}^{FD} \propto N^{1/2} \quad (12)$$

and k_{cy}^{ND} will always be larger than k_{cy}^{FD} except at very short chain lengths. Equation 12 leads to the prediction that in the absence of excluded volume $k_{cy}^{ND} \propto N^{-3/2}$.

Perico and Cuniberti[6] have become deeply involved in the question of end-to-end cyclization dynamics. These authors developed a method for calculating the exact eigenvalues of the hydrodynamic equation of a Rouse chain of finite length. By comparing these calculations with intrinsic viscosity measurements of various polymers in Θ solvents, they were able to describe each polymer in terms of two parameters—an effective scaling length related to chain flexibility and a hydrodynamic interaction parameter. Introducing these values into the Wilemski–Fixman theory permitted Perico and Cuniberti to calculate values

of k_{cy} for polystyrene and poly(dimethylsiloxane) for reasonable values of solvent viscosity and temperature. These values are reproduced in Table IV. A plot of their calculated k_{cy} values for polystyrene as log k_{cy} vs. log N shows a slope of −1.43.

Interpretation of k_{cy} Values. The results presented here pertain to polystyrene samples of $\bar{M}_n$ = 3000–30 000, i.e., a degree of polymerization of 30–300. Thus our highest molecular weight sample is somewhat lower in molecular weight than the lowest molecular weight for which Perico and Cuniberti predicted k_{cy} values.

Carrying out a slight extrapolation of either set of data leads to the conclusion that k_{cy} obtained from our experimental data is about a factor of 3 smaller than that predicted by Perico and Cuniberti.[6] The closeness of these values supports the validity of their model for hydrodynamic interactions of polymers of finite molecular weight. Clearly a more critical test of their model would involve determining k_{cy} in a Θ solvent.

It is somewhat disturbing that our experimental value of γ = 1.35 is lower than that predicted by all theoretical treatments of cyclization dynamics. Before one criticizes the theories for their inability to predict an experimental result, we must examine the experimental result critically in order to assess whether it is above question. First, γ is determined by a deconvolution process in which one measures a lifetime or emission intensity ratio for a polydisperse polymer. In deconvoluting the molecular weight dependence of the observations, we have difficulties assessing the magnitude of the standard deviation associated with our measure of γ. Second, we assumed that over our entire molecular weight range, k_{cy} could be described by a single parameter, $N^{-\gamma}$. We have some reason to suspect that this is not the case, and the net effect of this error would be to make the apparent absolute value of γ too small.

It is well documented that hydrocarbon chains of 8 to 16 carbons have difficulty cyclizing.[10] Cyclization is inhibited by transannular steric repulsions between methylene hydrogens. In polystyrene, these transannular repulsions are between phenyl rings. It would not be surprising if steric factors inhibited cyclization of polystyrene for rings of 30 or even 40 bonds. This is an important factor which must be assessed.

Our lowest molecular weight samples contain significant fractions of sufficiently low molecular weight polymer that cyclization of the chain ends in these fractions might be inhibited. The result would be excimer fluorescence intensities that were too low and pyrene fluorescence lifetimes that were too long. Hence we would underestimate k_{cy} values for our lower molecular weight samples. This would have the effect of making the apparent value of γ obtained from 6 lower than the "true" value.

We are unable to resolve this dilemma with the data reported here and are now directing our attention to similar experiments with much smaller molecular weight polydispersities.

Conclusions

Pyrene excimer formation is an excellent probe of the kinetics of end-to-end cyclization off terminally substituted polystyrene. The 200-ns pyrene fluorescence lifetime permits one to study, with a combination of steady-state and time-resolved measurements, rates of phenomena that occur even on the microsecond time scale. From the assumption that the rate constant for dynamically controlled end-to-end cyclization $k_{cy} \propto M^{-\gamma}$, we find that γ = 1.35. This value is smaller than that predicted by current theories of cyclization dynamics. Because k_{cy} is so sensitive to M, the value of γ is sensitive to the polydispersity of polymer samples used in the kinetic analysis. Future refinements of γ will require polymer samples of extremely narrow molecular weight distribution.

Acknowledgment. Acknowledgment is made to the donors of the Petroleum Research Fund, administered by the American Chemical Society, for partial support of this research. The authors also thank NSERC-Canada for its financial assistance. Special thanks are due to Dr. Paul Rempp and his research group at the CRM Strasbourg where he, Mr. Schuster, Dr. Lutz, Dr. Beinert, and Mr. Isel helped M.A.W. with the synthesis of the PS24K and PS27K polystyrene samples, as well as to Professor F. C. DeSchryver of the Katholeike Universiteit Leuven, who kindly permitted us to use his fluorescence spectrometers for our steady-state analyses. For helpful discussions we thank Professor De Schryver, Professor W. H. Stockmayer, Professor H. Morawetz, and Dr. Simon Fraser.

References and Notes

(1) (a) N. Goodman and H. Morawetz, *J. Polym. Sci., Part C*, **31**, 177 (1970); *J. Polym. Sci., Part A-2*, **9**, 1657 (1971); (b) J. A. Semlyen, *Adv. Polym. Sci.*, **21**, 41 (1976); (c) J. Chojnowski, M. Scibiorek, and J. Kowalski, *Makromol. Chem.*, **178**, 1351 (1977); (d) M. Sisido, E. Yoshikawa, Y. Imanishi, and T. Higashimura, *Bull. Chem. Soc. Jpn.*, **51**, 1464 (1978); (e) M. Sisido, H. Takgi, Y. Imanishi, and T. Higashimura, *Macromolecules*, **10**, 125 (1977); (f) H. Takagi, M. Sisido, Y. Imanishi, and T. Higashimura, *Bull. Chem. Soc. Jpn.*, **50**, 1807 (1977); (g) M. Sisido, T. Mitamura, Y. Imanishi, and T. Higashimura, *Macromolecules*, **9**, 316 (1976); (h) P. J. Flory and J. A. Semlyen, *J. Am. Chem. Soc.*, **88**, 3209 (1966); (i) H. Jacobsen and W. H. Stockmayer, *J. Chem. Phys.*, **18**, 1600 (1950); (j) H. Jacobsen, C. O. Beckman, and W. H. Stockmayer, *ibid.*, **18**, 1607 (1950).

(2) (a) F. C. DeSchryver, N. Boens, and J. Put, *Adv. Photochem.*, **10**, 359 (1977); (b) W. Klöpffer in "Organic Molecular Photophysics", Vol. I, J. B. Birks, Ed., Wiley, New York, 1973, p 357; (c) M. A. Winnik, *Acc. Chem. Res.*, **10**, 173 (1977); (d) G. Galli, G. Illuminati, L. Mandolini, and P. Tamborra, *J. Am. Chem. Soc.*, **99**, 2591 (1977); (e) G. Illuminati, L. Mandolini, and B. Masci, *ibid.*, **99**, 6308 (1977); (f) K. Shimada and M. Szwarc, *ibid.*, **97**, 3313, 3321 (1975); (g) K. Shimada, Y. Shimozato, and M. Szwarc, *ibid.*, **97**, 5834 (1975); (h) M. Yamamoto, K. Goshiki, T. Kanaya, and Y. Nishijima, *Chem. Phys. Lett.*, **56**, 333 (1978); (i) E. Haas, E. Katchalski-Katzir, and I. Z. Steinberg, *Biopolymers*, **17**, 11 (1978).

(3) (a) G. Wilemski and M. Fixman, *J. Chem. Phys.*, **58**, 4009 (1973); **60**, 866, 878 (1974); (b) M. Fixman, *ibid.*, **69**, 1527, 1538 (1978).

(4) (a) M. Doi, *Chem. Phys.*, **9**, 455–66 (1975); **11**, 107 (1975); (b) *ibid*, **11**, 115 (1975); (c) S. Sanagawa and M. Doi, *Polym. J.*, **7**, 604 (1975); **8**, 239 (1976); (d) M. Sakata and M. Doi, *ibid.*, **8**, 409 (1976).

(5) M. G. Brereton and A. Rusli, *Polymer*, **17**, 395 (1976).

(6) (a) A. Perico, P. Piaggio, and C. Cuniberti, *J. Chem. Phys.*, **62**, 4911 (1975); (b) A. Perico and C. Cuniberti, *J. Polym. Sci., Polym. Phys. Ed.*, **15**, 1435 (1977).

(7) C. Cuniberti and A. Perico, *Eur. Polym. J.*, **13**, 369 (1977).

(8) (a) J. B. Birks, "Photophysics of Aromatic Molecules", Wiley, New York, 1970, Chapter 7, p 301; (b) J. B. Birks, *Rep. Prog. Phys.*, **38**, 903 (1975).

(9) K. A. Zachariasse and W. Kühnle, *A. Phys. Chem. (Frankfurt am Main)*, **101**, 267 (1976).

(10) (a) G. M. Bennet, *Trans. Faraday Soc.*, **37**, 794 (1974); (b) M. Stoll and A. Rouvé, *Helv. Chim. Acta*, **17**, 1283, 1289 (1934); **18**, 1087 (1935).

(11) H. Ushiki, K. Horie, A. Okamoto, and I. Mita, submitted for publication. We thank Professor Mita for sharing his results with us prior to publication.

(12) K. H. Grellmann and H.-G. Scholz, *Chem. Phys. Lett.*, **62**, 64 (1979).

(13) L. H. Tung in "Gel Permeation Chromatography", K. H. Altgelt and L. Segal, Eds. Marcel Dekker, New York, 1971, p 145.

(14) W. R. Ware in "Creation and Detection of the Excited State", Vol. 1, A. Lamola, Ed., Marcel Dekker, New York, 1971, Chapter 5, p 213.

(15) S. G. Weissberg, R. Simha, and S. Rothman, *J. Res. Natl. Bur. Stand.*, **46**, 298 (1951). We are grateful to Professor H. Morawetz for bringing this paper to our attention.

(16) A similar equation was used to interpret intramolecular excimer formation by M. J. Goldenberg, J. Emert, and H. Morawetz, *J. Am. Chem. Soc.*, **100**, 7171 (1978).
(17) (a) G. Weill and J. des Cloizeaux, *J. Phys. (Paris)*, **40**, 100 (1979); (b) P. G. deGennes, *Macromolecules*, **9**, 587 (1976); (c) J. des Cloizeux, *J. Phys. (Paris), Colloq.*, **C2**, 135 (1978).
(18) J. L. Martin, M. S. Sykes, and F. T. Hioe, *J. Chem. Phys.*, **46**, 3478 (1967).
(19) P. H. Verdier and W. H. Stockmayer, *J. Chem. Phys.*, **36**, 227 (1962).

A Preliminary Examination of End Effects in Polyelectrolyte Theory: The Potential of a Line Segment of Charge

J. Skolnick* and Erik K. Grimmelmann

Bell Laboratories, Murray Hill, New Jersey 07974. *Received June 29, 1979*

ABSTRACT: The potential, ψ_T, of a line segment of charge is calculated in the Debye–Hückel approximation. We determine ψ_T as a function of segment length and the position of the test charge. If the test charge is near the line segment and the length of the line segment of charge is large relative to the screening length, ψ_T is well approximated by the electrostatic potential of an infinite line of charge. When the test charge is far from the line segment, ψ_T reduces to the point charge limit.

Recently, considerable attention has been devoted to elucidating the properties of the line of charge model of polyelectrolyte solutions.[1-6] The infinitely long line of charge model has been employed to calculate the colligative properties of dilute polyelectrolyte solutions,[1-3] the diffusion constant of a mobile ion in the presence of a polyelectrolyte,[4,5] and the expansion parameter, Z, of the excluded volume theory.[6] We note, however, that real polyions are of finite size; as such, it would be quite useful to determine the magnitude of end effects on the electrostatic potential arising from a finite line of charge. Hence, a partial motivation of the present work is to determine when the replacement of the potential of the line segment of charge by that of an infinite line is justified and when it is not. We also note that the line segment of charge may perhaps be a plausible model for low molecular weight DNA and helical poly(glutamic acid) at low to moderate ionic strengths. Thus, this paper is a preliminary step toward understanding the dependence of polyelectrolyte behavior on chain length.

If the length of the line segment of charge is large relative to the screening length and if the test charge is near the source, it seems intuitively reasonable that the electrostatic potential should be well approximated by the infinite line of charge result. However, when the test charge is far from the line segment of charge, the line segment should appear as a point charge. In the context of the Debye–Hückel approximation, verification of the above conjectures will be presented in what follows.

Consider a uniformly charged line segment of length L immersed in bulk solvent. It is assumed that each infinitesmal piece interacts with the test charge via a screened Coulomb potential. For discussions concerning the applicability of an effective charge density and counterion condensation, we refer to the literature.[1-3,7-9]

Let the line segment of charge lie on the z axis, in the cylindrical coordinate system (r,θ,z), and let one end of the line segment be located at $z = 0$. Whereupon, the potential, ψ_T, felt at a point $\mathbf{r} = (r,\theta,z)$ by a test charge is given by

$$\psi_T(\mathbf{r}) = \frac{\beta}{D_2}\int_0^L dz' \frac{\exp\{-\kappa[r^2 + (z - z')^2]^{1/2}\}}{[r^2 + (z - z')^2]^{1/2}} \quad (1)$$

* Address correspondence to this author at the Department of Chemistry, Louisiana State University, Baton Rouge, LA 70803.

with $\beta \equiv$ charge per unit length of the line segment and $D_2 \equiv$ bulk dielectric constant. κ^{-1} is the Debye screening length and is defined by

$$\kappa^2 = \frac{4\pi e^2}{D_2 k_B T}\sum_i C_i \mu_i^2$$

Here, e is the protonic charge. The summation extends over all the ionic species "i" in solution; C_i is the concentration of species "i" in ions per cm^3; μ_i is the valence of the ith species. k_B is Boltzmann's constant, and T is the absolute temperature.

It is convenient to define the dimensionless interaction energy ψ_d; ψ_d is related to ψ_T through the relation $\psi_d = \xi^{-1} e\psi_T/k_B T$; $\xi = |e\beta|/k_B T D_2$.

The test charge can either be positioned between the two ends of the line segment, i.e., $0 \le z \le L$, or below or above an end of the segment, i.e., $z < 0$ or $z > L$. By symmetry, it is obvious that the two latter situations are physically equivalent.

Let $z'' = z - z'$, it then follows from eq 1 that

$$\psi_d(\mathbf{r}) = \int_{-z}^{L-z} dz'' \frac{\exp\{-\kappa[r^2 + z''^2]^{1/2}\}}{[r^2 + z''^2]^{1/2}} \quad (2)$$

If $0 \le z \le L$,

$$\psi_d = \int_0^{L-z} dz'' \frac{\exp\{-\kappa[r^2 + z''^2]^{1/2}\}}{[r^2 + z''^2]^{1/2}} + \int_0^z dz'' \frac{\exp\{-\kappa[r^2 + z''^2]^{1/2}\}}{[r^2 + z''^2]^{1/2}} \quad (3)$$

Similarly when $z < 0$

$$\psi_d{}^b = \int_0^{L+|z|} dz'' \frac{\exp\{-\kappa[r^2 + z''^2]^{1/2}\}}{[r^2 + z''^2]^{1/2}} - \int_0^{|z|} dz'' \frac{\exp\{-\kappa[r^2 + z''^2]^{1/2}\}}{[r^2 + z''^2]^{1/2}} \quad (4)$$

While it is apparent from eq 3 and 4 that the potential ψ_d must vary continuously from the $0 \le z \le L$ case to that when $z < 0$, we find it conceptually useful to examine the two situations separately. As the $0 \le z \le L$ configuration is most closely related to the infinite line result, it is treated first.

At this juncture, a few qualitative observations on certain limiting forms of ψ_d are necessary. First of all, it must

0024-9297/80/2213-0335$01.00/0